Ecological Modelling 290 (2014) 121–133

Contents lists available at ScienceDirect

Ecological Modelling

journal homepage: www.elsevier.com/locate/ecolmodel

A new probabilistic canopy dynamics model (SLCD) that is suitable for evergreen and deciduous forest ecosystems

J. Sainte-Marie[a,b,*], L. Saint-André[b,c], Y. Nouvellon[c,f], J.-P. Laclau[c,e], O. Roupsard[c,d], G. le Maire[c], N. Delpierre[g], A. Henrot[a], M. Barrandon[a]

[a] Université de Lorraine, UMR Institut Elie Cartan, F-54506 Vandoeuvre-lès-Nancy, France
[b] INRA, Biogéochimie des Ecosystèmes Forestiers, F-54280 Champenoux, France
[c] CIRAD, UMR Eco&Sols, F-34060 Montpellier, France
[d] CATIE, Tropical Agricultural Research and Higher Education Center, 7170 Turrialba, Costa Rica
[e] Departamento Recursos Naturais, Universidade Estadual de São Paulo, UNESP, Botucatu, SP 18610-307, Brazil
[f] USP, Universidade de São Paulo, ESALQ, Departamento de Ciências Atmosféricas, IAG, CEP 05508-900 São Paulo, Brazil
[g] Univ. Paris-Sud, Laboratoire Ecologie Systématique et Evolution, UMR8079, Orsay F-91405, France

ARTICLE INFO

Article history:
Available online 16 February 2014

Keywords:
Climate changes
Canopy dynamics
Probabilistic model
Process-based model (PBM)
Growth & yield model (G&YM)

ABSTRACT

There are strong uncertainties regarding *LAI* dynamics in forest ecosystems in response to climate change. While empirical growth & yield models (G&YMs) provide good estimations of tree growth at the stand level on a yearly to decennial scale, process-based models (PBMs) use *LAI* dynamics as a key variable for enabling the accurate prediction of tree growth over short time scales. Bridging the gap between PBMs and G&YMs could improve the prediction of forest growth and, therefore, carbon, water and nutrient fluxes by combining modeling approaches at the stand level.

Our study aimed to estimate monthly changes of leaf area in response to climate variations from sparse measurements of foliage area and biomass. A leaf population probabilistic model (SLCD) was designed to simulate foliage renewal. The leaf population was distributed in monthly cohorts, and the total population size was limited depending on forest age and productivity. Foliage dynamics were driven by a foliation function and the probabilities ruling leaf aging or fall. Their formulation depends on the forest environment.

The model was applied to three tree species growing under contrasting climates and soil types. In tropical Brazilian evergreen broadleaf eucalypt plantations, the phenology was described using 8 parameters. A multi-objective evolutionary algorithm method (MOEA) was used to fit the model parameters on litterfall and *LAI* data over an entire stand rotation. Field measurements from a second eucalypt stand were used to validate the model. Seasonal *LAI* changes were accurately rendered for both sites ($R^2 = 0.898$ adjustment, $R^2 = 0.698$ validation). Litterfall production was correctly simulated ($R^2 = 0.562$, $R^2 = 0.4018$ validation) and may be improved by using additional validation data in future work. In two French temperate deciduous forests (beech and oak), we adapted phenological sub-modules of the CASTANEA model to simulate canopy dynamics, and SLCD was validated using *LAI* measurements. The phenological patterns were simulated with good accuracy in the two cases studied. However, LAI_{max} was not accurately simulated in the beech forest, and further improvement is required.

Our probabilistic approach is expected to contribute to improving predictions of *LAI* dynamics. The model formalism is general and suitable to broadleaf forests for a large range of ecological conditions.

1. Introduction

Global changes lead to increases in environmental stresses in forest ecosystems. Forest managers have to define forestry policies that combine economic constraints and ecosystem sustainability. Improving our comprehension of the factors that influence the global functioning of forest ecosystems is a major challenge in addressing global changes. Modeling tools are to be improved to explicitly account for both silvicultural practices and the environment in the predictions of forest productivities. A multi-disciplinary approach is suggested by Reyer et al. (2013) to assess vegetation responses to global changes.

Saint-André (2013) classified the current modeling approaches in forest science into three disciplinary classes, highlighting their strengths and limitations:

* Corresponding author at: Institut Elie Cartan, Université de Lorraine, B.P. 70239, 54506 Vandoeuvre-lès-Nancy Cedex, France. Tel.: +33 03 83 68 45 90.
E-mail address: juliensaintemarie@gmail.com (J. Sainte-Marie).

0304-3800/$ – see front matter © 2014 Elsevier B.V. All rights reserved.
http://dx.doi.org/10.1016/j.ecolmodel.2014.01.026

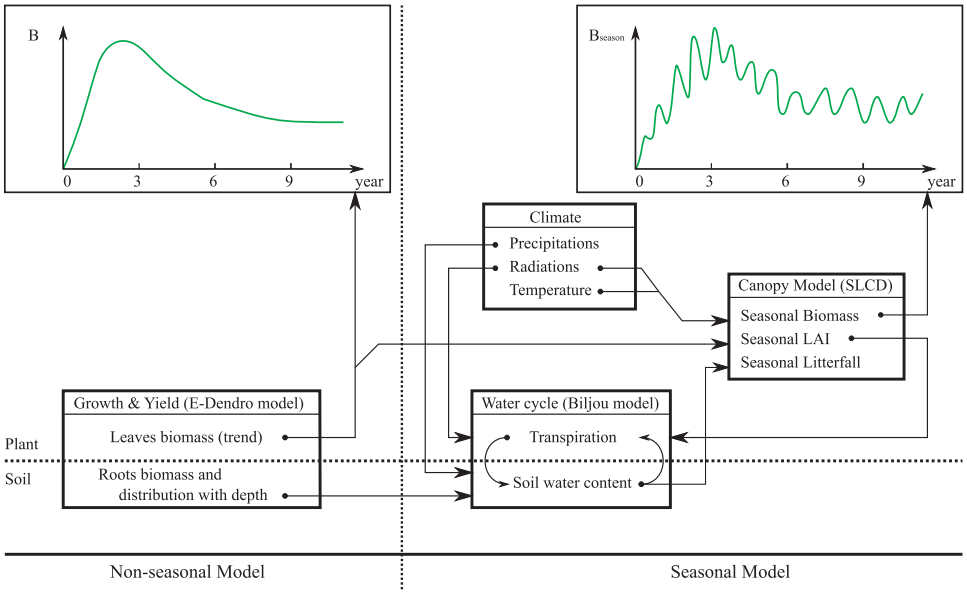

Fig. 1. Flowchart of the integrative modeling approach used to introduce seasonality in growth & yield models and assessing the influence of stand growth, foliar biomass and climate on the water cycle. The model combination was focused on eucalypt plantations and combines the growth & yield model E-DENDRO, the process-based model of stand transpiration BILJOU and the Stand Leaf Canopy Dynamics model (SLCD). Climatic data drive both the BILJOU and SLCD. There is feedback between BILJOU and SLCD: the seasonal leaf area index (*LAI*) is an input of BILJOU and drives the forest transpiration rate and, thus, the soil water content; then, the drought stress (*DS*) is calculated and used in SLCD. This feedback provides a description of the influence of forest growth, climate and foliage dynamics on the water cycle. The work presented in this article focused on SLCD calibration. *DS* was obtained from measurements. Future work will focus on the combination of BILJOU and SLCD.

- forestry and biometry with growth and yield models (G&YMs) such as FAGACEES (Dhote, 1996) or E-DENDRO (Saint-André et al., 2002; Saint-André et al., 2005; Saint-André et al., 2008). These empirical models accurately estimate wood production and nutrient allocation within tree components, are relevant over long periods of time and account for silvicultural practices. However, climate, water cycling and the biogeochemical cycles of nutrients are not explicitly considered. Their use is limited to the sites and climates considered for the calibration, which is likely to considerably limit their use in the context of climate change.
- ecophysiology using process-based models (PBMs) such as CASTANEA (Dufrene et al., 2005; Davi et al., 2005), G'DAY (Corbeels et al., 2005a,b; Marsden et al., in press), BILJOU (Granier et al., 1999) or BALANCE (Roetzer et al., 2010). These mechanistic models simulate the coupling of carbon and water cycles. They explicitly consider the climate but exhibit poor performance in simulations of the effects of silvicultural practices on biomass allocation within tree components.
- biogeochemistry and soil chemistry models such as SAFE (Sverdrup et al., 2006), FORSVA (Arp and Oja, 1997; Oja and Arp, 1997) or FORNBM (Zhu et al., 2003a,b)). These models provide a consistent description of soil biogeochemical processes (mineral weathering, soil organic matter mineralization and soil solution chemistry). However, the description of nutrient uptake and dry matter allocation within trees is still under development.

These approaches consider a large variability in spatial and temporal scales, which implies that a simple juxtaposition is not sufficient to model the functioning of the whole ecosystem. It is therefore necessary to establish new modeling strategies to assess forest sustainability under various climatic and silvicultural scenarios. This idea is already applied in the model FORSAFE in the context of biochemistry (Wallman et al., 2005) or in the global vegetation model ORCHIDEE (Bellassen et al., 2010, 2011). These works highlight the large number of interactions between cycles, which generate feedback effects that are difficult to model.

The Stand Leaf Cohorts Dynamics (SLCD) model was developed in the context of improving G&YMs (Sainte-Marie et al., 2012). We expect that introducing climate, phenology and biogeochemical cycles in these models can improve their capacity to simulate soil–plant interactions and tree growth, along with considering management practices and changes in the environment. Modeling of canopy phenology is an essential step towards the development of comprehensive models that include water and nutrient balances in the predictions of tree growth. SLCD aims to (1) provide relevant estimations of seasonal *LAI* to drive PBM such as BILJOU (Granier et al., 1999); (2) introduce phenology in foliar biomass estimations provided by G&YMs such as FAGACEES (beech) and E-DENDRO (eucalypt); and (3) estimate the amounts of leaf production and litterfall. This paper focuses on phenology and does not consider the coupling of models. The association between G&YMs, PBMs and phenological estimations forms the basis for further works. However, to illustrate our global modeling method, we propose an example of models combined with flowcharts dedicated to *eucalypt* plantations (Fig. 1).

Foliage dynamics play a key role in PBMs (e.g., G'DAY, CASTANEA). PBM simulations of carbon sequestration and tree growth are very sensitive to leaf area index (*LAI*) variations and require reliable estimations of *LAI* to be used over long time periods. *LAI* is used to drive forest transpiration models (e.g., Shuttleworth and Wallace (1985), Chouhury and Monteith (1988), Granier et al. (1999), Fisher et al. (2009), Jung et al. (2010)) and to determine the fraction of photosynthetically active radiation (*PAR*) absorbed by the vegetation (e.g., Gower et al. (1999), Nouvellon et al. (2000)). *LAI* can be measured in various ways (Breda, 1999), as follows: direct estimations by destructive sampling (Nouvellon et al., 2010), indirect estimations by satellite remote sensing (le Maire et al., 2011) or using optical devices such as LAI2000 (Licor) or hemispherical photographs.

In addition to the issue of the *LAI* estimate, litterfall production is the main organic matter input in decomposition models (e.g., Bosatta and Agren (1996), d'Annunzio et al. (2008)). Litterfall simulation is essential for enabling further modeling developments that incorporate nutrient cycling.

Chabot and Hicks (1982) and Kikuzawa and Lechowicz (2011) showed that canopy renewal can be considered the result of

forest growth optimization and carbon-use efficiency. Therefore, the optimization of photosynthetic activity would be driving canopy dynamics through rapid changes in leaf expansion and leaf mortality rates. In this approach, each leaf has a photosynthetic potential that declines over time (Kitajima et al., 1997, 1997, 2002). Senescence processes are initiated if the leaf photosynthetic potential is lower than the cost of leaf attachment. Independent of this optimization theory, abiotic stresses such as frost (Silva et al., 2009) and drought (Chabot and Hicks, 1982) and biotic stresses such as herbivory (Lowman and Heatwole, 1992) are likely to cause premature leaf fall or disappearance.

Recently, phenology modeling was initiated under climate change pressure and is still under development (Richardson et al., 2013). While climatic factors driving boreal and temperate phenology are well identified, the modeling of tropical phenology is poorly studied and understood. Satellite data-based studies (Botta et al., 2000; Jolly et al., 2005; Stoeckli et al., 2008) proposed global climatic indicators to predict phenology. Simple climatic indexes are associated with climatic variables (vapor pressure deficit, photoperiod, minimum temperature) and are used to identify the most limiting factor in canopy dynamics.

In this study, we aimed to simulate *LAI* dynamics and litterfall at the stand level with a modeling tool that takes advantage of the large diversity of modeling approaches in forest science. We developed a new method to simulate *LAI* dynamics and litterfall production based on sparse measurements taken on a few days. We hypothesized that a simple probabilistic model (hereafter named SLCD) based on monthly leaf cohort dynamics had sufficient flexibility for accurately simulating *LAI* dynamics and litterfall production for both fast-growing evergreen plantations and deciduous temperate forests. SLCD is, by construction, designed to enable further developments by considering feedback from water and nutrient cycles. SLCD includes functions that consider leaf appearance, growth and fall, thereby accounting for the environment.

Our modeling approach was applied at three sites covered by tropical evergreen eucalypt plantations in Brazil and temperate deciduous forest in France essentially composed of beech (Hesse site) and oak (Barbeau site).

2. Materials & methods

2.1. Description of the SLCD model

Table 1 provides a summary of the model variables.

2.1.1. Model inputs

According to G&YM time scales, SLCD has a monthly time step $k \in \mathbb{N}^*$ for the stand age, but to ensure a connection with PBMs such as BILJOU, we used daily climatic data to drive the leaf phenology. The time variable d is used when daily data are considered.

The required climatic data for each site are detailed below.

In addition, to account for the advantages of growth and yield models (sound principles based upon Eichhorn's rule, Assmann's yield level theory and Langsaeter hypothesis), the trend of biomass with stand age (denoted B), without seasonal variations, is used as an input variable in the SLCD model (Fig. 1). Information on the individual leaf mass (m) and individual leaf surface (s) is required to estimate the model outputs. These data were obtained from measurements in this study and may depend on leaf age (see Section 2.2.3) and forest age.

2.1.2. Leaf population dynamics

Foliage turnover is a combination of three successive processes: (1) bud burst/leaf emergence; (2) leaf expansion; and (3) leaf senescence/abscission. SLCD considers the foliage to be a population of leaves that are distributed by monthly classes of age i named cohorts. Leaf age is defined as the difference between the current month and budburst month. After falling, the age of the leaf is defined as the duration between emergence and abscission. Note that the age i of a leaf is always less than or equal to the stand age k.

Table 1
List of variables, types (T), symbols and units used to execute and calibrate SLCD. The variables are classified in 3 types: I, input variable; S, state variable; and O, output variable. Variables with no type specified are mentioned in the article but not explicitly used in SLCD.

Variable	T	Symb.	Unit
(a) Climate and soil water			
Daily mean temperature	I	T	°C
Drought stress	I	DS	–
Global radiation	I	R_g	$MJ\,m^{-2}\,month^{-1}$
Monthly mean temperature	I	T_m	°C
Photosynthetic active radiation	I	PAR	$MJ\,m^{-2}\,month^{-1}$
Photoperiod	I	π	$h\,day^{-1}$
Relative extractable water	I	REW	–
(b) Canopy			
Foliar biomass trend	I	B	$kg\,m^{-2}$
Leaf mass	I	m	kg_{leaf}
Leaf mass area	I	LMA	$kg_{leaf}\,m^{-2}_{leaf}$
Leaf mean mass	I	$\bar{m}$	kg_{leaf}
Leaf mean surface	I	$\bar{s}$	m^2_{leaf}
Specific leaf area	I	SLA	$m^2_{leaf}\,kg^{-1}_{leaf}$
Dead leaf population of age i	S	N^i_F	leaf
Leaf population	S	N	leaf
Leaf age	S	i	month
Leaf population of age i	S	N^i	leaf
Maximal leaf population	S	N_{max}	leaf
Production pressure on leaf fall	S	δ	–
Space available for new leaves	S	θ	leaf
Stand age	S	k	month
Seasonal foliar biomass	O	B_{season}	$kg\,m^{-2}$
Leaf area index	O	LAI	$m^2_{leaf}\,m^2_{soil}$
Litterfall	O	LF	$kg\,m^{-2}$
Normalized Difference Vegetation Index	–	$NDVI$	–
Plant area index	–	PAI	$m^2_{vegetation}\,m^2_{soil}$

The population $N(k) \in \mathbb{N}$ of leaves carried by the forest at month k is given by

$$N(k) = \sum_{i \geq 1} N^i(k) \tag{1}$$

where $N^i(k) \in \mathbb{N}$ is the number of leaves of age i at month k. We also introduced the number $N^i_F(k)$ of leaves of age i that fell during month k. Seasonal simulations of foliar biomass (B_{season}), litterfall (LF) and leaf area index (LAI) are obtained by coupling cohort dynamics and single-leaf surface and mass.

Two successive modeling steps, for each month k, are used to model cohorts' dynamics (Fig. 2). The iteration of these two steps establishes a probabilistic dynamic model for the foliage demography. This model is a branching process with immigration (Harris, 1963; Olofsson, 1996).

2.1.2.1. Leaf mortality. It is necessary to determine the probability that each leaf is abscised or maintained on the tree. A probability is assigned to each cohort, and the *fall probability* for a leaf of age i at month k is denoted $p^i_F(k)$.

For each study site, a phenological hypothesis is required to define fall probabilities that may depend on leaf age, forest age, senescence processes and climatic and environmental variables. A major issue is determining how to formalize and combine all of these factors.

First, a function named *fall index* is defined for each phenological process involved in leaf fall. Each fall index function generates a real

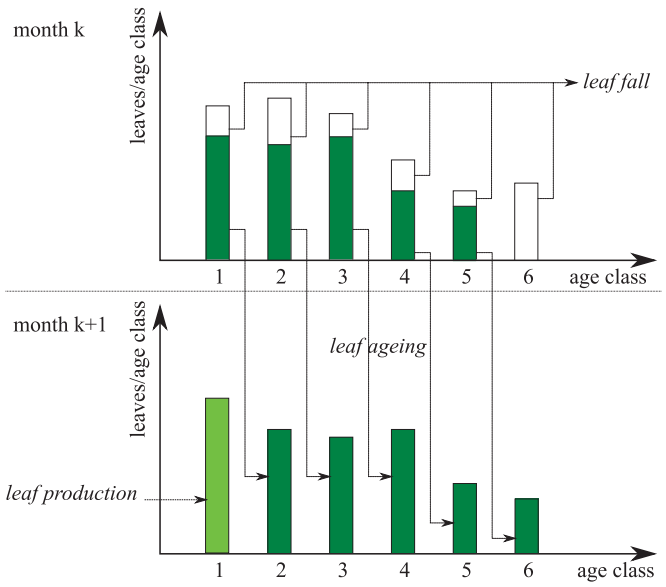

Fig. 2. Iterative process of the SLCD model. Successive processes driving canopy dynamics are denoted in italics. Leaf fall and aging result from fall probabilities. The creation of new leaves occurs after leaf aging, when the total number of leaves still attached has been estimated. Leaf production is driven by the non-seasonal biomass time series B given by growth & yield models and the foliation function φ.

number included in [0, 1]. The number and the type of functions vary among the study sites (see below).

Second, fall indexes are combined to define the fall probability. For a cohort of age i, let us consider q fall indexes $(p_j^i(k))_{j\in\{1,q\}}$. Then, the probability $p_F^i(k)$ is defined as follows:

$$p_F^i(k) = f(p_1^i(k), p_2^i(k), \ldots, p_q^i(k)), \tag{2}$$

where $f: [0, 1]^q \to [0, 1]$ is the *combinatory function* defined as follows:

$$f(p_1, \ldots, p_q) = 1 - \prod_{j=1}^{q} \left(1 - p_j^{\alpha_j}\right). \tag{3}$$

The positive real numbers $\alpha_1, \ldots, \alpha_q$ are parameters used during model fitting to optimize the combination of fall indexes. The combinatory function satisfies

$$\text{if it exists } j \in \{0, q\} \text{ such that } p_j^i = 1, \text{ then } f(p_1^i, \ldots, p_q^i) = 1. \tag{4}$$

This property ensures leaf fall if a lethal event occurs (i.e., at least one fall index is equal to one).

The number of leaves $N^i(k)$ of age $i \geq 2$ is obtained from the population $N^{i-1}(k-1)$ using the binomial law $\mathcal{B}\left(N^{i-1}(k-1), p_F^{i-1}(k-1)\right)$. This law also provides the number of fallen leaves $N_F^{i-1}(k-1)$, which satisfies the following equality:

$$N_F^{i-1}(k-1) + N^i(k) = N^{i-1}(k-1). \tag{5}$$

2.1.2.2. Leaf production. The production of new leaves $N^1(k)$ is determined for each month k. First, we assume that the total number of leaves attached in the forest crown is limited by the crown size. Second, we assume that the *maximal number of leaves* is linked to the trend of stand foliar biomass per meter square $B(k)$. Let us denote the maximal number of leaves that can hold forest crown as $N_{max}(k)$. Depending on the season, the total population $N(k)$ may be lower than or equal to $N_{max}(k)$.

We also define the mean leaf mass $\bar{m}(k)$ as follows:

$$\overline{m}(k) = \sum_{i\leq 1} \frac{N^i(k) m(i, k)}{N(k)}. \tag{6}$$

Then, the term $B(k)/\overline{m}(k)$ corresponds formally to a number of leaves, and we assume its proportionality with $N_{max}(k)$. Because $B(k)/\overline{m}(k)$ is an average estimate of the leaves held in the tree crown, $N_{max}(k)$ may exceed $B(k)/\overline{m}(k)$. Thus, we introduce the positive constant λ, and then

$$N_{\max}(k) = \lfloor \lambda \frac{B(k)}{\overline{m}(k)} \rfloor, \tag{7}$$

where $\lfloor . \rfloor$ is the nearest integer function.

Then, it is possible to define the *space available for new leaves*. It is denoted as θ and is calculated as the difference between the maximal number of leaves and the total number of leaves attached to the trees:

$$\theta(k) = \max\left(0, N_{\max}(k) - \sum_{i\geq 2} N^i(k)\right). \tag{8}$$

It is necessary to determine when this available space is filled with new leaves. To integrate our assumptions on leaf creation processes, we define a *foliation function*, denoted as φ (see Sections 2.2.4 and 2.3.1). It expresses the proportion of the available space used to create new leaves. Its value is included in [0, 1] and depends on our foliation assumptions. When the environmental conditions are more favorable to foliation, the value of φ is higher. The combination of θ and φ yields the production of young leaves:

$$N^1(k) = \lfloor \theta(k)\, \varphi(k) \rfloor. \tag{9}$$

The expression $N^1(k)$ (Eq. (9)) is a feedback loop influenced by environmental conditions. The maximal number of leaves constrains the leaf production by saturation of the tree crown.

2.1.3. Model outputs

To obtain B_{season}, *LAI* and *LF*, we used information on the mean leaf mass (m) and surface (s) in every cohort:

$$B_{season}(k) = \sum_{i\geq 1} N^i(k)\, m(k, i), \tag{10}$$

$$LAI(k) = \sum_{i\geq 1} N^i(k)\, s(k, i), \tag{11}$$

$$LF(k) = \sum_{i\geq 1} N_F^i(k)\, m(k, i). \tag{12}$$

If information on m or on s are lacking, additional variables such as the leaf mass area (*LMA*) can be used to fill in the missing data as follows:

$$m(k, i) = LMA(k)\, s(k, i) = \frac{s(k, i)}{SLA(k)}. \tag{13}$$

2.2. Tropical evergreen eucalypt plantations

Over the last twenty years, the intensive monitoring of biomass dynamics in eucalypt plantations (Laclau et al., 2000; Stape et al., 2004) has led to the design of several biomass models (e.g., E-DENDRO (Saint-André et al., 2002), G'DAY (Corbeels et al., 2005a) and CABALA (Battaglia et al., 2004)). The biomass predictions of these models combined with leaf traits and SLCD may contribute to the improvement of the PBMs used to manage these plantations (Fig. 1).

This article considers the phenology of Brazilian eucalypt plantations. A review was used to establish parametric functions simulating leaf emergence and abscission. Parameters were fitted on monthly litterfall measurements and remote sensing estimates of *LAI* (see Laclau et al. (2010), le Maire et al. (2011) and le Maire et al. (2013) for details). Given the high number of parameters, a multi-objective evolutionary algorithm method (MOEA) was chosen for model fitting (Van Veldhuizen and Lamont, 2000). Model validation was performed for an independent data set obtained from a second stand situated nearby.

2.2.1. Study site 1: Eucalyptus, Itatinga, Brazil

The Itatinga Experimental Station (23°02′ S and 48°38′ W) is covered with *Eucalyptus grandis* (W. Hill ex Maiden) plantations. The mean annual rainfall spanning the 15 years before our study was 1360 mm. The average annual temperature was 20 °C. The seasonal cold period occurred from June to September, with an absolute minimum of 4.8 °C recorded in July 2000, along with minimum temperature values below 5 °C for a few days each year. The relief was typical of the western plateau of São Paulo, with a gentle wavy topography. The experimental site was located on a hilltop (slope <3%) at an altitude of 850 m. The soils were very deep Ferralsols (>15 m) developed on Cretaceous sandstone, Marília formation, Bauru group, with a clay content ranging from 14% in the A1 horizon to 23% in deep soil layers. This study focused on two experimental plantations, E101 and E137, as described in Laclau et al. (2009) and le Maire et al. (2013), respectively. The same mono-progeny of *E. grandis* seedlings was planted in April 2004 in E101 and May 2003 in E137. The stocking density was slightly lower in E137 than in E101 (1111 vs 1666 trees ha^{-1}), and nitrogen (N) fertilizers were not applied in E137, whereas they were applied at 120 kg N ha^{-1} for the first 1.5 years after planting in E101. The other silvicultural practices were similar in the two experiments. The positive effect of fertilizers on biomass production was only significant the first two years after planting at our study site, and the total aboveground biomass produced was similar in E101 and E137 at the end of the rotation (unpublished data).

2.2.2. Climatic and environmental data

Global radiation (R_g) measurements were obtained from UNESP university at Botucatu (30 km from the study site). Other climatic data used in SLCD were measured at the Itatinga experimental station (a distance <1 km from the E101 and E137 experimental sites).

An estimate of the monthly drought stress *DS* was defined based on the soil water content measurements. Its definition is based on the daily relative extractable water (*REW*). *REW* is the ratio between the amount of water available in soil and the maximal amount of water extractable from the soil.

REW was computed from soil water content measurements collected every 1–7 days down to a depth of 3 m with TDR probes (Time Domain Reflectometry, Trase soil moisture, CA, USA). Granier et al. (1999) defined a critical threshold $REW_c = 0.4$ under which the ecosystem is submitted to drought limitation. Each day d in month k, if $REW(d,k) \geq REW_c$, the daily drought stress is $REW_c - REW(d,k)$. *DS* on month k is defined as the sum of daily stresses occurring in month k:

$$DS(k) = \sum_{d \in month(k)} \max(0, REW_c - REW(d,k)). \quad (14)$$

2.2.3. Foliage measurements

The same methodology was used to estimate stand *LAI* in E101 and E137 and is fully described in Laclau et al. (2010).

Measurements of B_{season} and *LAI* were obtained once a year at the end of the rainy season, with destructive sampling over the 6 years of the rotation cycle. An additional measurement was performed seven months after planting. The variations in *LAI* were interpolated between these annual *LAI* field measurements using satellite images, as in le Maire et al. (2013). Briefly, MODIS reflectances in red and NIR wavebands, at a resolution of 250 m and a frequency of 16 days, have been used to invert a canopy reflectance model and retrieve *LAI*, as in le Maire et al. (2011). The MODIS pixel chosen in the present study belongs to a large eucalyptus stand of the same age and clonality, which was near the E101 experimental site. This inverted *LAI* time series was then normalized to fit the annual field measurements taken in E101 (see le Maire et al. (2013)). As a consequence, the seasonal dynamics of *LAI* between two field measurements could be estimated fairly well.

LF was collected monthly.

Changes in leaf mass throughout the leaf life span were measured in E101 by Laclau et al. (2010) for our *E. grandis* seedlings, which led to the following empirical relationship:

$$m(i) = 3.5 \times 10^{-4} \left(1 - e^{-0.82.i}\right), \quad (15)$$

where i is the monthly leaf age.

SLA was estimated in E101 annually at the end of each rainy season from destructive measurements of *LAI* using the following relationship:

$$SLA = \frac{LAI}{B}. \quad (16)$$

Missing monthly data were predicted using a cubic spline interpolation.

2.2.4. Phenology and model formulation

2.2.4.1. Leaf production. In tropical evergreen forests, radiation peaks and drought effects were identified as the major driving force behind the tropical ecosystem phenology (Bradley et al., 2011). Monitoring of Australian eucalypt forests (Pook, 1984a,b, 1985; Pook et al., 1997) highlighted a strong correlation among leaf production, leaf loss and water availability.

We assumed that drought stress slowed foliation. When the drought stress *DS* exceeded a critical threshold DS_{crit}, foliation decreased proportionally to *DS*. The foliation function φ was given by the following expression:

$$\varphi(k) = \begin{cases} 1, & \text{if } DS(k) \leq DS_{crit}, \\ \max(0, 1 - \nu_{DS}(DS(k) - DS_{crit})), & \text{else}, \end{cases} \quad (17)$$

where ν_{DS} and DS_{crit} were two positive parameters to be adjusted.

Wright and Van Schaick (1994) also associated leaf production to peaks of irradiance. Simulations including this effect were also performed, with poor results (unpublished data).

2.2.4.2. Leaf aging. Leaf traits are influenced by seasonality, forest age and nutrient availability (Hikosaka, 2005; Laclau et al., 2009; Pornon et al., 2011). *SLA* decreases with tree age (England and Attiwill, 2006; Nouvellon et al., 2010), which corresponds to an increase in self-shading in the crown. The dynamics of the SLA values measured in E101 over the entire rotation period exhibited this tendency. Variations in the leaf mass m are given by Eq. (15).

2.2.4.3. Leaf fall. According to the carbon balance optimization theory, a favorable light regime speeds up leaf fall (Reich et al., 2004; Vincent, 2006). Moreover, photosynthesis is enhanced during favorable temperature periods (Battaglia et al., 1998), which accelerate leaf fall.

Self-shading among leaves was observed in tropical forests (Ackerly and Bazzaz, 1995; Ackerly, 1999) and eucalypt plantations (Whitehead and Beadle, 2004). An increase in *LAI* led to an increase in self-shading, which delayed leaf fall at the bottom of the crown.

This vertical gradient is associated with an increase in leaf thickness at the bottom of the crown. Thus, the variability in the leaf lifespan was influenced by the leaf position in the crown, and a faster renewal of foliage occurred at the top of canopy.

Reductions in stomatal conductance during droughts slow down photosynthetic activity and delay leaf fall (Kikuzawa and Lechowicz, 2011), while severe droughts cause litterfall peaks. Under water shortage conditions, leaf shedding seems to be a complex and adaptative behavior to hydrous stress: a study of the eucalypt response to two drought periods Pook (1986) showed that the trees protected themselves by promptly shedding some of their leaves.

We define a unique fall index p_{R_g} for the effect of radiation on leaf fall, calculated as the quantity of energy received by the tree crown at month k i months ($i \leq k$) from the time series of R_g. The Beer–Lambert law for radiation extinction through the canopy was used to estimated the influence of *LAI* on the amount of energy received. We assume that drought stress reduces the energy received. We define the amount of energy absorbed by the foliage at month k over a period of i months as follows:

$$E^i(k) = \sum_{j=k-i}^{k} \frac{R_g(j)(1 - e^{-0.48\,LAI(j)})}{1 + \beta_{DS} DS(j)}, \tag{18}$$

where β_{DS} is a parameter to be fit. The extinction coefficient value (0.48) was determined based on previous studies (Roupsard et al., 2008). We assume that the effect of radiation on leaf fall increased proportionally with the energy received. Furthermore, the leaf traits changed over the whole rotation. Because *SLA* decreased in both experiments, the leaves were thicker at the end of the rotation. According to the carbon balance optimization theory, we assume that the thick leaves positioned at the bottom of tree crown were more likely to have a higher lifespan than thinner leaves.

In addition, litterfall peaks were observed when *LAI* increased. We assume that new incoming leaves were accelerating the fall of older leaves. Rather than using a simple difference in *LAI* values between two successive months, we estimated the production pressure on litterfall (noted δ) using

$$\delta(k) = \frac{LAI(k)}{B(k)\,SLA(k)} - \frac{LAI(k-1)}{B(k-1)\,SLA(k-1)}. \tag{19}$$

The product $B \times SLA$ is equivalent to a leaf area index trend depending on the plantation age. We chose to divide *LAI* by *B* and *SLA* to normalize the variations in *LAI*. δ is an index without unit.

Finally, we assume that a minimal amount of energy E_{min} had to be reached before leaf fall occurred and that the fall index p_{R_g} was defined by

$$p^i_{R_g}(k) = \min(1,\ \beta_{R_g} \quad \max(0\,,\ 1 + \beta_{PP}\,\delta(k-1))\ldots \\ SLA(k)\ \max(0, E^i(k) - E_{\min})), \tag{20}$$

where β_{R_g} and E_{min} were two parameters to be fit.

2.2.5. Model fitting

Model fitting was performed on a dataset collected from E101. We simulated an entire rotation from the first leaf fall one year after planting, in April 2005, to a few months before harvesting in September 2009.

2.2.5.1. Input variables. The model was designed to be driven by the biomass time series *B* given by a G&YM. When these data were missing, we replaced them by a time series that had the same features, namely, the stand age-related estimates of foliar biomass without seasonal variations. We chose to set *B* as the annual measurements of B_{season} and to predict missing data using cubic spline interpolation. Considering the annual gap between measurements and the regularity of the splines, the obtained time series *B* was assumed to be equivalent to the G&YM predictions.

Surfaces of leaves *s* were obtained each month using Eq. (15) and *SLA* estimates.

Table 2
Model adjustment results (Site 1): parameter values, research interval & units.

Param.	Value	Res. int.	Unit
λ	1.0563	[1, 1.3]	–
ν_{DS}	0.2203	[0, 1]	–
DS_{crit}	1.5709	[0, 8]	–
β_{DS}	0.7544	[0, 10]	–
β_{PP}	7.4423	[0, 10]	–
β_{R_g}	2.5493×10^{-5}	$[0, 5 \times 10^{-4}]$	$kg_{leaf}\,MJ^{-1}$ month
E_{min}	308.17	$[0, 10^4]$	$MJ\,m^{-2}$ $month^{-1}$
αR_g	1.3310	[0, 10]	–

2.2.5.2. Fitting method. Model fitting was performed on *LF* and *LAI* measurements simultaneously. We selected an objective to minimize for each one:

$$\|LAI_{mea} - LAI_{sim}\|_2 = \left(\sum_{k=1}^{n} (LAI_{mea}(k) - LAI_{sim}(k))^2\right)^{1/2}, \tag{21}$$

$$\|LF_{mea} - LF_{sim}\|_4 = \left(\sum_{k=1}^{n} (LF_{mea}(k) - LF_{sim}(k))^4\right)^{1/4}, \tag{22}$$

where $n = 72$ was the number of measurements. A classical l^2 norm was tested, and the resulting *LF* flushes were underestimated. We chose to consider the l^4 norm for *LF* for simulations considering the large *LF* flushes.

The existence of a unique group of parameters minimizing both objectives simultaneously was very unlikely. Indeed, a group of parameters minimizing one objective may not necessarily minimize the other. Thus, the notion of Pareto efficiency was used to determine the set of simulations that was considered to be the best compromise among the objectives to minimize. The set of simulations that were Pareto efficient, i.e., the set of best compromises, is called the Pareto front. A genetic algorithm method was used to evaluate the Pareto front. This method described by Van Veldhuizen and Lamont (2000) is classified as a multi-objective evolutionary algorithm method (MOEA) and is implemented in the MATLAB optimization toolbox.

Eight parameters were fitted with multi-objective optimization. Three parameters were related to foliation: λ, ν_{DS} and DS_{crit}. A single fall index for radiation effect p_{R_g} was defined by 4 parameters: β_{DS}, β_{R_g}, β_{PP} and E_{min}. Recall that a combinatory function (Eq. (3)) introduced an additional parameter α_{R_g}. We used this parameter to optimize model fitting, although a unique fall index was defined. Each parameter was researched in a relevant interval with regard to the associated variables (Table 2).

The Pareto front was obtained, and the efficiency of the simulations (R^2) for both *LAI* and *LF* was considered to exclude irrelevant groups of parameters. Finally, we selected the best estimate of the cumulative *LF* production over the whole rotation.

2.2.5.3. Model validation. The methodology used to determine model inputs was identical to that used in the E101 experiment. The fitted set of parameters was tested on the dataset collected in E137 from 36 to 59 months after planting. The lack of *REW* data shortened the validation period.

2.3. Deciduous temperate ecosystems

In the case of French forests, monthly leaf production, expansion and fall probability were established using phenological sub-modules of the daily-based PBM CASTANEA. The parameters used were taken from previous studies (Davi et al., 2008; Delpierre, 2009; Delpierre et al., 2009), and no calibration was required. These simulations aimed to assess the formalism suitability of SLCD and its compatibility with PBMs and daily-based models. SLCD validation was performed on LAI_{max} (beech) and foliage dynamics measurements (beech and oak).

2.3.1. Phenology and model formulation

In deciduous temperate ecosystems, foliation and senescence are essentially triggered by variations in the photoperiod. The influence of the latter depends on altitudinal and temperature gradients. A warm spring accelerates foliation processes, and senescence is favored by cold autumnal temperatures. Water availability is also a limiting factor (Delpierre et al., 2009; Fracheboud et al., 2009; Lebourgeois et al., 2008; Vitasse et al., 2009a, 2009, 2009c).

2.3.1.1. Bud burst. Delpierre (2009) defined a three-parameter model to determine the date of bud burst.

The end of winter dormancy day was noted as $D_{startBB}$. After this date, the model considers the daily mean temperature T exceeding the base temperature T_{baseBB}:

$$R_{BB}(d) = T(d)\,\mathbb{1}_{\{T(d)\geq T_{baseBB}\}}, \tag{23}$$

and cumulates them:

$$S_{BB}(d) = \sum_{j=D_{startBB}}^{d} R_{BB}(j). \tag{24}$$

The date of bud burst D_{BB} is obtained when S_{BB} reaches the critical value F_{critBB}.

This daily CASTANEA sub-model was used to define the foliation function with a simple formulation:

$$\varphi(k) = \mathbb{1}_{\{D_{BB}\in month(k)\}}. \tag{25}$$

2.3.1.2. Leaf expansion. Davi et al. (2008) described the CASTANEA sub-model used to simulate leaf expansion.

The leaf growth was assumed to be proportional to the cumulative daily temperature after bud burst. The full expansion is reached when the sum equals the critical value $F_{critexp}$:

$$S_{\exp}(d) = \min\left(F_{critexp}, \sum_{j=D_{BB}}^{d} T(j)\right). \tag{26}$$

The value used in the SLCD model for leaf expansion each month is the value of the ratio $S_{exp}/F_{critexp}$ at the end of the month.

2.3.1.3. Leaf senescence. The CASTANEA senescence sub-model was described by Delpierre et al. (2009).

Senescence processes are initiated when the daily photoperiod $\pi(d)$ is lower than a threshold $\pi_{startsen}$. It defines the day $D_{startsen}$ that corresponds to the beginning of senescence processes.

$$R_{sen}(d) = (T_{basesen} - T(d))^{x}\left(\frac{\pi(d)}{\pi_{startsen}}\right)^{y}\mathbb{1}_{\{T(d)<T_{startsen}\}} \tag{27}$$

$$S_{sen}(d) = \min\left(F_{critsen}, \sum_{j=D_{startsen}}^{d} R_{sen}(j)\right) \tag{28}$$

Table 3
Parameters of the CASTANEA sub-models used for sites 2 and 3: parameters, values, & origin.

Parameter	Site 2	Site 3	Unit	Source
(a) Bud burst				
$D_{startBB}$	91	55	day	Delpierre (2009)
T_{baseBB}	4.6	4	°C	Delpierre (2009)
F_{critBB}	190	410	°C	Delpierre (2009)
(b) Leaf expansion				
$F_{critexp}$	424	424	°C	Davi et al. (2008)
(c) Leaf senescence				
$\pi_{startsen}$	12.5	14.5	day	Delpierre et al. (2009)
$T_{basesen}$	25	26.5	°C	Delpierre et al. (2009)
x	2	2	–	Delpierre et al. (2009)
y	2	0	–	Delpierre et al. (2009)
$F_{critsen}$	5160	10,178	°C	Delpierre et al. (2009)

The value used in the SLCD model for the monthly fall index p_{sen} is the value of the ratio $S_{sen}/F_{critsen}$ at the end of the month.

2.3.2. Beech, Hesse, France (site 2)

2.3.2.1. Site description. The experimental plot was located in the state forest of Hesse, France (48°40′ N, 7°05′ E, elevation 300 m), which was (90%) composed of beech (*Fagus sylvatica L.*). The other tree species present were *Carpinus betulus*, *Betulaalba*, *Fraxinus excelsior*, *Prunus avium*, *Quercus petraea* and *Larix decidua*. The understorey vegetation was very sparse. The annual precipitation was 820 mm, and the average annual temperature was 9.2 °C. The soil type was intermediate between a luvisol and a stagnic luvisol. The clay content ranged between 25 and 35% within a 0–100 cm depth and was approximately 40% below 100 cm. A complete description of the site is given by Granier et al. (2000).

2.3.2.2. Input data. Climatic data required to perform simulations included the calculated daily photoperiod π (method described by Allen et al. (1998)) and the daily mean temperature T obtained from in situ flux towers (Longdoz, personal communication).

In the case of deciduous forests, the spring foliar biomass production equals the autumnal litterfall. In the case of the Hesse site, annual LF measurements were recorded. Because the study focused on phenological phases in French sites, we chose to define B based on annual LF measurements.

The leaf mean surface at full expansion (10.7 cm^2 $leaf^{-1}$) and the mean LMA (80 g m^{-2}) were measured (Granier, Personal communication). Eq. 13 was used to determine the leaf mean mass $\overline{m}$ at full expansion.

2.3.2.3. Model validation. Foliage dynamics were simulated from January 1997 to December 2008. The model performance was assessed using the maximal annual LAI measurements and estimates of forest cover dynamics. The parameters used in the phenological functions are given in Table 3.

The forest cover dynamics was estimated using the Plant Area Index (PAI). PAI was estimated using the inversion of the Beer–Lambert law for radiation absorption $R_g^{soil} = R_g \quad \exp(-k_{R_g} \times PAI)$. Daily radiations at the soil level R_g^{soil} and above the tree crown R_g were obtained from in situ flux towers. The maximal values of PAI_{max} were modified to compare the phenology of the measured PAI and the simulated LAI.

2.3.3. Oak, Barbeau, France (site 3)

2.3.3.1. Site description. The plot is located in Barbeau, France (48°28′ N, 2°46′ E) and is composed of oak (*Q. petraea*). The annual precipitation was 670 mm, and the average annual temperature was 10.8 °C. The soil type was a leached soil with pseudogley. The clay content was 15% within a 0–30 cm depth and was

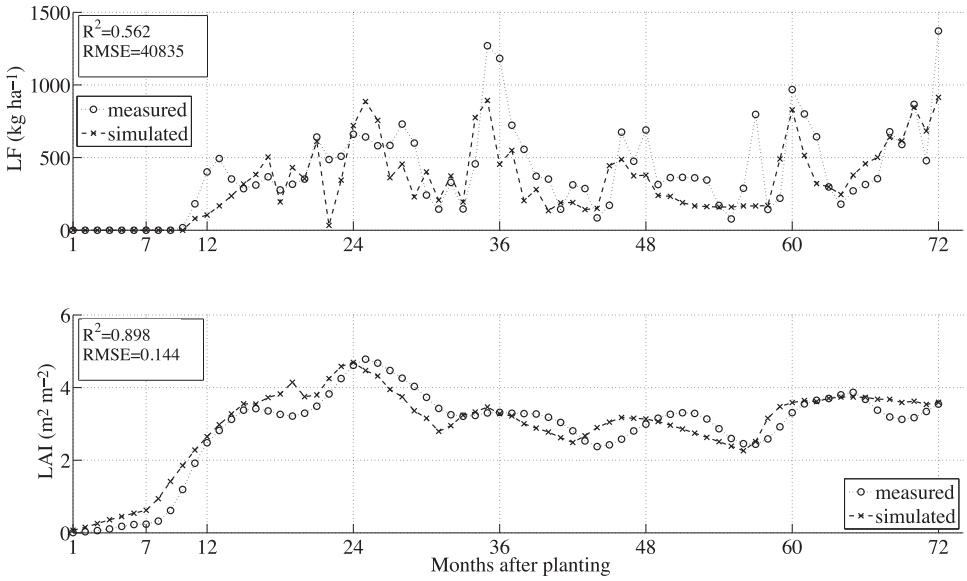

Fig. 3. Comparison of the measured and simulated data in the E101 plantation (site 1) over the whole rotation: litterfall (*LF*) (above) and leaf area index (*LAI*) (below).

approximately 30% for the entire profile. The site is described by Delpierre (2009).

2.3.3.2. Input data. The climatic data required to perform simulations were the calculated daily photoperiod π (method described in Allen et al. (1998)) and the daily mean temperature T obtained from in situ flux towers.

In this study site, no *LF* data were obtained to measure the foliar biomass trend B. The annual maximal *LAI* values were obtained from measurements (2009) and modeling results (2006–2008). The annual B was estimated using the relationship:

$$B = LAI_{\max} LMA. \quad (29)$$

Davi et al. (2008) obtained *LMA* from a top canopy LMA_{max} measurement and a Beer–Lambert extinction profile equation depending on *LAI* and the extinction coefficient $k_{LMA} = 0.187$:

$$LMA = LMA_{\max} \frac{1 - e^{-k_{LMA} LAI}}{k_{LMA} LAI}. \quad (30)$$

The leaf traits mean leaf surface (20.37 cm^2 $leaf^{-1}$) and LMA_{max} (105 g cm^{-2}) were measured.

2.3.3.3. Model validation. Foliage dynamics were simulated from January 2005 to December 2009. The parameters used in the phenological functions are given in Table 3. The model performance was assessed using measurements of *PAI* dynamics. Using a similar method as that used for site 2, *PAI* data were calculated from measurements of *PAR* extinction through the tree crown.

3. Results

3.1. Eucalyptus, Itatinga, Brazil (Site 1)

3.1.1. Model adjustment

Eight parameters were fitted on the E101 stand data (Table 2). *LAI* was simulated with good accuracy ($R^2 = 0.898$, $RMSE = 0.144$). *LAI* was slightly overestimated (2.8%).

The periodicity of *LAI* was well simulated, with a slight decay between the measured and simulated time series (Fig. 3).

LF was rendered with lower accuracy ($R^2 = 0.562$, $RMSE = 40835$). The total *LF* production over the whole rotation was underestimated by 17.8%, due to inaccurate estimations for a few months (the 12th, 36th and 57th). The measured *LF* followed an annual pattern marked by annual peaks since the age of 36 months. A similar pattern was observed in the *LF* simulations over the whole rotation (Figs. 3 and 4).

The simulated annual mean leaf lifespan increased from 3.1 months between 1 and 12 months after planting to 9.06 months between 49 and 60 months after planting. A lower mean lifespan (5.5 months) was simulated between 61 and 72 months after planting.

The simulated annual maximal leaf lifespan increased from 15 months during the first year after planting (the seedlings were five months old at the time of planting) to 32 months during the 6th year after planting. These elevated values were related to small leaf populations remaining attached to trees for several years.

3.1.2. Model validation

The periodicity of the *LAI* predictions ($R^2 = 0.698$, $RMSE = 0.449$) was respected over the validation period (Fig. 5). The average *LAI* simulated over the whole validation period was 4.27, compared to 4.06 for the average measurements, representing an overestimation of 6.55%. The amplitude of the simulated *LAI* time series was smaller than the measured amplitude of *LAI* (Fig. 6).

The periodicity of the *LF* production peaks was respected ($R^2 = 0.4018$, $RMSE = 221.41$). Two production peaks around the 37th and 57th months were overestimated, and the total *LF* production was overestimated by 37% over the whole validation period.

3.2. Beech, Hesse, France (Site 2)

The measured yearly maximal *LAI* was well estimated in most cases. However, it was strongly overestimated in 2006 (35.32%) and underestimated in 1998 and 2008 (18.25 and 14.29 %, respectively). Smaller differences were observed in 1999, 2001 and 2007 (Fig. 8).

Measurements of the *LAI* dynamics exhibited a gap in 2000, 2001, 2002, 2003 and 2005 (Fig. 7). In the remaining years, the *LAI* dynamics simulations corresponded to the measurements, except in 1998 and 1999, where an offset of one month was observed in senescence. Besides, the leaf emergence and growth were simulated with good accuracy.

The data highlighted two *LAI* increase phases. The first phase was fast and simulated accurately. The second phase was slow

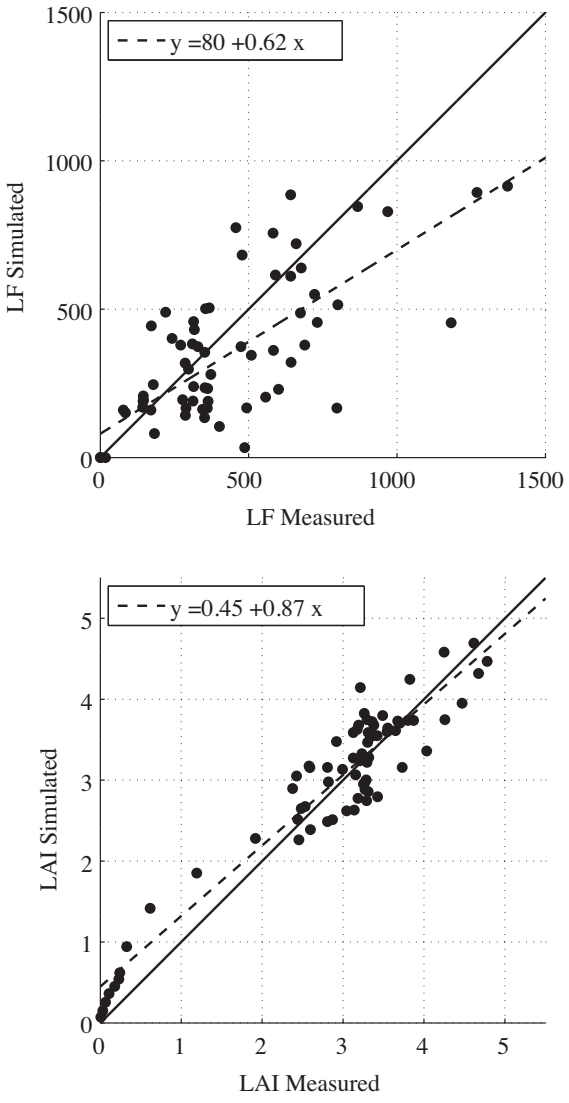

Fig. 4. Comparison of the measured and simulated data in the E101 stand (site 1): first-order linear regression for litterfall (*LF*) (above) and leaf area index (*LAI*) (below).

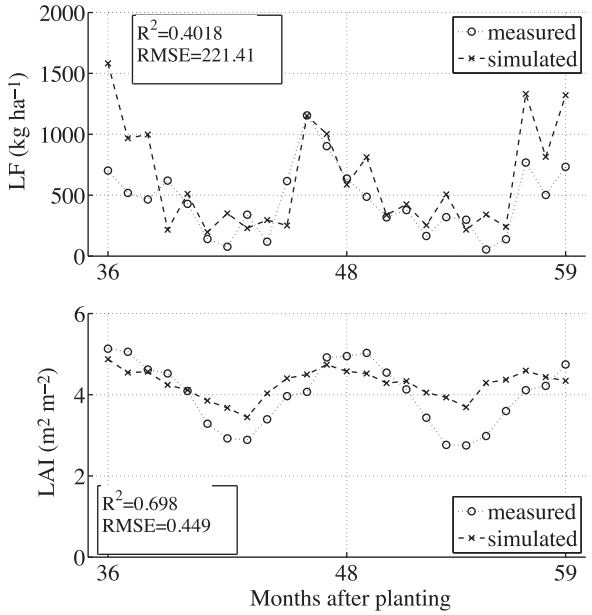

Fig. 5. Comparison of the measured and simulated data in the E137 stand (site 1): litterfall (*LF*) (above) and leaf area index (*LAI*) (below).

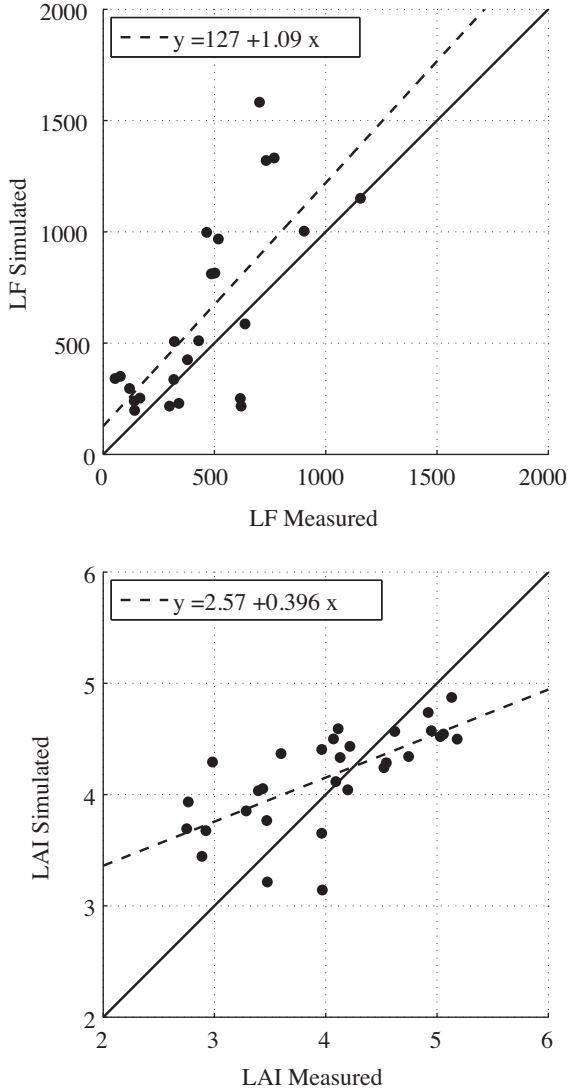

Fig. 6. Comparison of the measured and simulated data in the E137 plantation (site 1): first-order linear regression for litterfall (*LF*) (above) and leaf area index (*LAI*) (below).

and occurred between May and October in most years. This phenomenon was not taken into account in the simulation.

3.3. Oak, Barbeau, France (Site 3)

The bud burst and leaf growth patterns were respected. A one-month delay was observed in leaf senescence in 2006 and 2007 (Fig. 9).

4. Discussion

4.1. Evergreen eucalypt plantation (Brazil)

Several attempts were made to determine the most influent factors involved in the phenology of these plantations.

Limiting effects on foliation due to low temperatures and low radiation levels were tested, as was the water availability effect. We finally excluded these effects, which did not specifically improve the simulations. The main factor driving foliation is the water availability, as suggested by Pook's studies (Pook, 1984a,b, 1985; Pook et al., 1997).

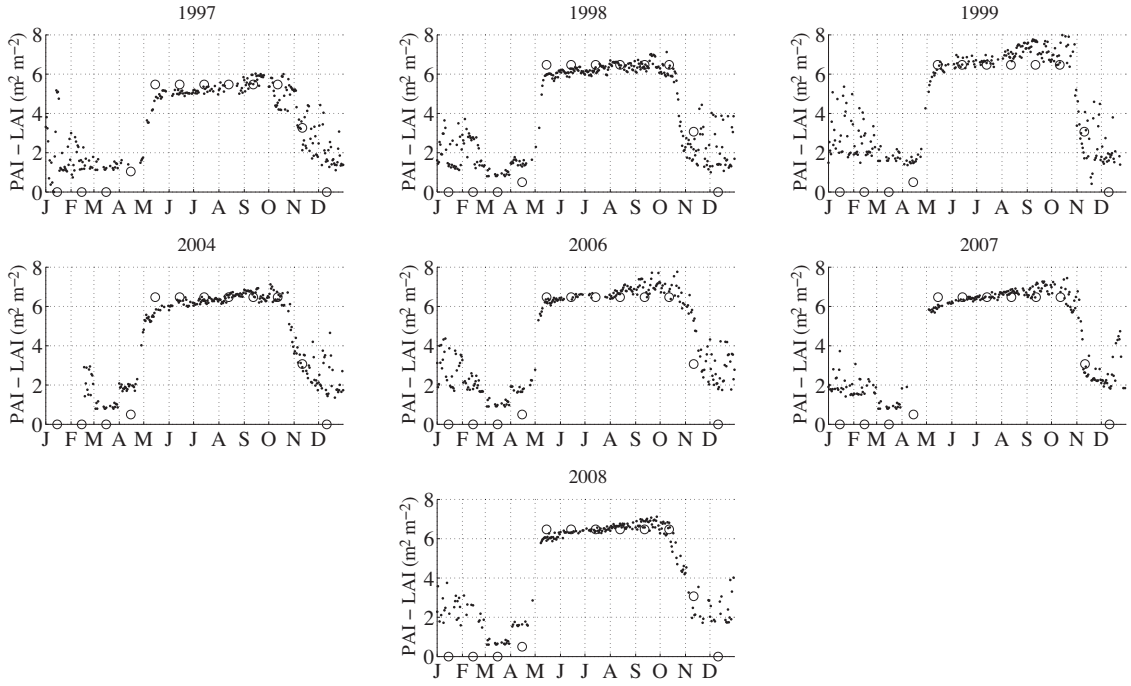

Fig. 7. Comparison of the plant area index (*PAI*) dynamics measurements (•) and simulated leaf area index (*LAI*) (○) in site 2.

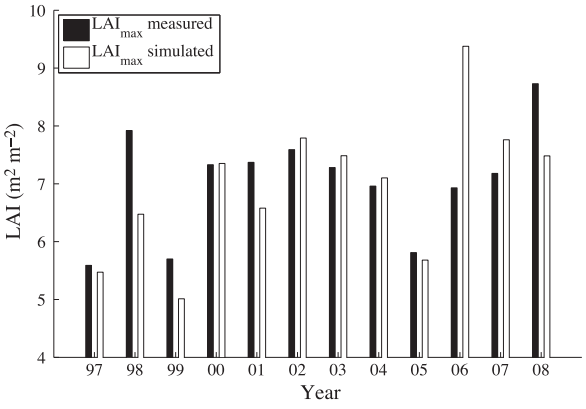

Fig. 8. Comparison of the measured and simulated annual maximal values of the leaf area index (*LAI*) in site 2. An elevated difference was observed in 1998, 2006 and 2008.

A unique fall index was used in this study. This restriction was due to the limited amount of validation data. Nevertheless, a second fall index related to severe drought was tested (unpublished data) and used to simulate the *LF* peak, which occurred in the 57th iteration after planting on the E101 stand (Fig. 3). An extended validation set is required to validate this fall index. An estimation of the soil water content over the whole E137 experimental site using the BILJOU model is ongoing work. Note that the combinatory function (Eq. (3)) was tested and was sufficient for introducing additional fall indexes.

Our model then confirmed that the effects of both radiation (leaf fall) and drought (foliation and leaf fall) were the major driving forces behind tropical ecosystem phenology. It also highlighted a strong internal regulation process of phenology. Indeed, *LAI* was used to determine both the fraction of energy absorbed by the tree crown (Eq. (18)) and the production pressure on litterfall (Eq. (19)). Several possibilities without internal regulation processes were unsuccessfully tested to estimate the impact of radiation on *LF*. Some modeling attempts were also performed without considering the influence of a decrease in *SLA* on p_{R_g}, with poor results for both *LAI* and *LF*.

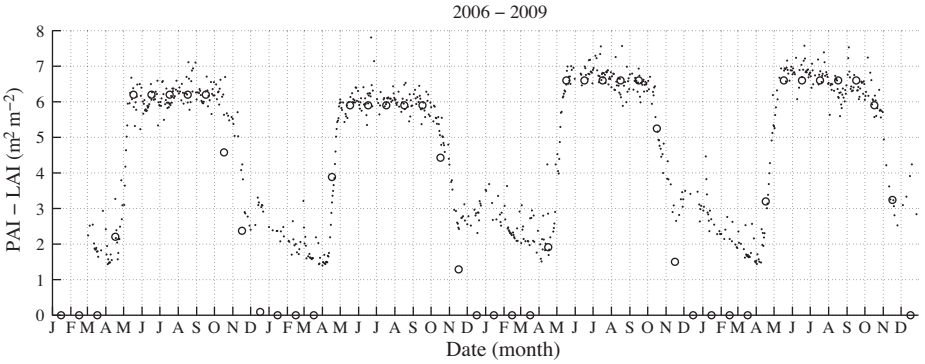

Fig. 9. Comparison of the plant area index (*PAI*) dynamics measurements (•) and simulated leaf area index (*LAI*) (○) between 2006 and 2009 in site 3. The phenology was well predicted, except in autumn 2006, when the senescence occurred too early for prediction.

Variations in the mean leaf lifespan correspond to the results obtained by Laclau et al. (2009), which were close to the values calculated using the 3-PG model (Almeida et al., 2004). Elevated leaf maximal ages (>1 year) have been reported in the literature. Whitehead and Beadle (2004) cited several studies on eucalypt native forests, where a substantial portion of leaves survived for up to 18 month or 2 years. In the case of *Eucalyptus maculata* native forests, some leaves survived up to 3 years (Pook, 1984a).

The E101 and E137 experimental sites were strongly fertilized, and nitrogen and potassium fertilization regimes influenced the leaf longevity and leaf traits (Laclau et al., 2009). Further improvements in SLCD require investigations addressing the role of tree nutrition on leaf longevity. In addition, the lower stocking density in E137 than in E101 influenced the crown architecture, and the resulting consequences on leaf longevity deserve further attention.

4.2. Deciduous ecosystem (France)

From the point of view of the SLCD formalism, considering deciduous ecosystems was easier than considering evergreen ecosystems. The phenological phases were clear, and a simple adaptation of the phenological sub-modules of CASTANEA model was sufficient to render the phenology with good accuracy in both cases.

However, shifts in the maximal *LAI* simulation were observed in the Hesse site. In this case, differences in the LAI_{max} simulations can be attributed to the constant leaf traits used during the whole simulation.

4.3. Model development

In the case of the evergreen ecosystems, the phenology is difficult to model. One strength of our approach is simultaneously estimating litterfall production and *LAI* variations using a formulation that incorporates the tree physiology. We expect that our model may be used to determine the main processes involved in leaf production and the net primary production of evergreen ecosystems.

This study highlights the need to investigate the interaction between foliage and nutrient cycling to improve the SLCD model. Indeed, SLCD is strongly sensitive to leaf traits, which are strongly influenced by nutrient availability (Hikosaka, 2005; Pornon et al., 2011). In addition, the impact climate on leaf traits has to be considered (Wright et al., 2005).

Due to its formalism, SLCD can be further enhanced with future investigations. It is possible to perform model coupling with biogeochemical models in a manner similar to coupling with PBM. Thus, introduction of the role of nutrients in foliage dynamics is possible in the general modeling framework presented in the Introduction to this paper.

In every study site, *LAI* was simulated with a good accuracy. Because stand transpiration is driven by *LAI* in a PBM such as BILJOU, the efficiency of SLCD is sufficient for performing a combination of models, as shown in Fig. 1. In the case of deciduous ecosystems, our study is in the preliminary phase of coupling G&YM FAGACEES, PBM BILJOU and SLCD. Because SLCD predictions are dependent on the annual foliar biomass estimation, the accuracy of such a coupling will strongly depend on annual biomass estimations given by FAGACEES.

The development of a complex model results in an increase in the number of required parameters. Furthermore, a complete monitoring of forest ecosystems is rare. Thus, modelers often face the issue of sparse data from various compartments of a forest ecosystem. Our study demonstrates that MOEAs are able to fit complex models based on several variables. Recent developments in MOEAs indicate good prospects for the future development of complex forest ecosystem models.

5. Conclusion

The SLCD model was designed for use in a coupling of models, combining the advantages of G&YMs and PBMs at the stand level. In Brazilian eucalypt plantations, *LAI* and *LF* were globally predicted with good accuracy and may be improved by using complementary validation data and introducing the influence of climate and nutrients on leaf traits. In deciduous forest ecosystems, the suitability of the model formalism was established with the successful introduction of phenological sub-modules of the CASTANEA model. In every case, SLCD opens new perspectives in the development of a new generation of soil–plant models.

Acknowledgements

The authors would like to thank André Granier and Bernard Longdoz for their help in the study of the Hesse data.

This article was given financial support by “Ministère de l’enseignement supérieur et de la recherche”, “Université de Lorraine” and “Office National des Forêt”. This work was supported by a grant overseen by the French National Research Agency (ANR) as part of the “Investissements d’Avenir” program (ANR-11-LABX-0002-01, Lab of Excellence ARBRE), the European community (CARBOAFRICA, CLIMAFRICA) and the French national network SOERE F-ORE-T.

References

Ackerly, D., 1999. Self-shading, carbon gain and leaf dynamics: a test of alternative optimality models. Oecologia 119 (May (3)), 300–310.
Ackerly, D.D., Bazzaz, F.A., 1995. Leaf dynamics, self-shading and carbon gain in seedlings of a tropical pioneer tree. Oecologia 101 (March (3)), 289–298.
Allen, R.G., Pereira, L.S., Raes, D., Smith, M., 1998. Crop evapotranspiration: guidelines for computing crop water requirements. FAO Irrigation and Drainage Paper (56), xxvi + 300 pp.-xxvi + 300 pp.
Almeida, A.C., Landsberg, J.J., Sands, P.J., 2004. Parameterisation of 3-pg model for fast-growing eucalyptus grandis plantations. Forest Ecology and Management 193 (May (1–2)), 179–195.
Arp, P.A., Oja, T., 1997. A forest soil vegetation atmosphere model (forsva). 1. Concepts. Ecological Modelling 95 (2–3), 211–224.
Battaglia, M., Cherry, M., Beadle, C., Sands, P., Hingston, A., 1998. Prediction of leaf area index in eucalypt plantations: effects of water stress and temperature. Tree Physiology 18 (8–9), 521–528.
Battaglia, M., Sands, P., White, D., Mummery, D., 2004. Cabala: a linked carbon, water and nitrogen model of forest growth for silvicultural decision support. Forest Ecology and Management 193 (May (1–2)), 251–282.
Bellassen, V., le Maire, G., Dhote, J., Ciais, P., Viovy, N., 2010. Modelling forest management within a global vegetation model. Part 1: Model structure and general behaviour. Ecological Modelling 221 (October (20)), 2458–2474.
Bellassen, V., le Maire, G., Guin, O., Dhote, J., Ciais, P., Viovy, N., 2011. Modelling forest management within a global vegetation model. Part 2: Model validation from a tree to a continental scale. Ecological Modelling 222 (January (1)), 57–75.
Bosatta, E., Agren, G., 1996. Theoretical analyses of carbon and nutrient dynamics in soil profiles. Soil Biology and Biochemistry 28 (10–11), 1523–1531.
Botta, A., Viovy, N., Ciais, P., Friedlingstein, P., Monfray, P., 2000. A global prognostic scheme of leaf onset using satellite data. Global Change Biology 6 (7), 709–725.
Bradley, A., Gerard, V.F., Barbier, F., Weedon, N., Anderson, G.P., Huntingford, L.O., Aragao, C., Zelazowski, L.E.O.C., Arai, P.E., 2011. Relationships between phenology, radiation and precipitation in the Amazon region. Global Change Biology 17 (June (6)), 2245–2260.
Breda, N., 1999. The leaf area index of forest canopies: measurement, variability and functional role. Revue Forestiere Francaise 51 (2), 135–150.
Chabot, B.F., Hicks, D.J., 1982. The ecology of leaf life spans. Annual Review of Ecology and Systematics 13, 229–259.
Chouhury, B.J., Monteith, J.L., 1988. A 4-layer model for the heat-budget of homogeneous land surfaces. Quarterly Journal of The Royal Meteorological Society 114 (480), 373–398.
Corbeels, M., McMurtrie, R., Pepper, D., O’Connell, A., 2005a. A process-based model of nitrogen cycling in forest plantations. Part I. Structure, calibration and analysis of the decomposition model. Ecological Modelling 187 (4), 426–448.
Corbeels, M., McMurtrie, R., Pepper, D., O’Connell, A., 2005b. A process-based model of nitrogen cycling in forest plantations. Part II. simulating growth and nitrogen mineralisation of eucalyptus globulus plantations in South-Western Australia. Ecological Modelling 187 (4), 449–474.
d’Annunzio, R., Zeller, B., Nicolas, M., Dhote, J.F., Saint-Andre, L., 2008. Decomposition of European Beech (Fagus sylvatica) litter: combining quality theory and n-15 labelling experiments. Soil Biology and Biochemistry 40 (2), 322–333.

Davi, H., Barbaroux, C., Dufrene, E., Francois, C., Montpied, P., Breda, N., Badeck, F., 2008. Modelling leaf mass per area in forest canopy as affected by prevailing radiation conditions. Ecological Modelling 211 (March (3–4)), 339–349.

Davi, H., Dufrene, E., Granier, A., Le Dantec, V., Barbaroux, C., Francois, C., Breda, N., 2005. Modelling carbon and water cycles in a beech forest. Part II: Validation of the main processes from organ to stand scale. Ecological Modelling 185 (July (2–4)), 387–405.

Delpierre, N., 2009. Etude du déterminisme des variations interannuelles des échanges carbonés entre les écosystèmes forestiers européens et l'atmosphère: une approche basée sur la modélisation des processus (Ph.D. thesis). Université Paris XI.

Delpierre, N., Dufrene, E., Soudani, K., Ulrich, E., Cecchini, S., Boe, J., Francois, C., 2009. Modelling interannual and spatial variability of leaf senescence for three deciduous tree species in France. Agricultural and Forest Meteorology 149 (6–7), 938–948.

Dhote, J.F., 1996. A model of even-aged beech stands productivity with process-based interpretations. Annales des Sciences Forestières 53 (1), 1–20.

Dufrene, E., Davi, H., Francois, C., le Maire, G., Le Dantec, V., Granier, A., 2005. Modelling carbon and water cycles in a beech forest. Part I: Model description and uncertainty analysis on modelled nee. Ecological Modelling 185 (July (2–4)), 407–436.

England, J.R., Attiwill, P.M., 2006. Changes in leaf morphology and anatomy with tree age and height in the broadleaved evergreen species, Eucalyptus regnans F. muell. Trees: Structure and Function 20 (1), 79–90.

Fisher, J., Malhi, Y., Bonal, D., Rocha, H.R.d., Araujo, A.C.d., Gamo, M., Goulden, M., Hirano, T., Huete, A., Kondo, H., Kumagai, T., Loescher, H., Miller, S., Nobre, A., Nouvellon, Y., Oberbauer, S., Panuthai, S., Roupsard, O., Saleska, S., Tanaka, K., Tanaka, N., Tu, K., Randow, C.v., 2009. The land-atmosphere water flux in the tropics. Global Change Biology 15 (11), 2694–2714.

Fracheboud, Y., Luquez, V., Bjorken, L., Sjodin, A., Tuominen, H., Jansson, S., 2009. The control of autumn senescence in European aspen. Plant Physiology 149 (4), 1982–1991.

Gower, S.T., Kucharik, C.J., Norman, J.M., 1999. Direct and indirect estimation of leaf area index, f(apar), and net primary production of terrestrial ecosystems. Remote Sensing of Environment 70 (October 1), 29–51.

Granier, A., Biron, P., Lemoine, D., 2000. Water balance, transpiration and canopy conductance in two beech stands. Agricultural and Forest Meteorology 100 (4), 291–308.

Granier, A., Breda, N., Biron, P., Villette, S., 1999. A lumped water balance model to evaluate duration and intensity of drought constraints in forest stands. Ecological Modelling 116 (2–3), 269–283.

Harris, T.E., 1963. The Theory of Branching Processes. Die Grundlehren der Mathematischen Wissenschaften, Bd. 119. Springer-Verlag/Prentice-Hall, Inc., Berlin/Englewood Cliffs, N.J, xiv+230 pp.

Hikosaka, K., 2005. Leaf canopy as a dynamic system: ecophysiology and optimality in leaf turnover. Annals of Botany 95 (3), 521–533.

Jolly, W.M., Nemani, R., Running, S.W., 2005. A generalized, bioclimatic index to predict foliar phenology in response to climate. Global Change Biology 11 (4), 619–632.

Jung, M., Reichstein, M., Ciais, P., Seneviratne, S.I., Sheffield, J., Goulden, M.L., Bonan, G., Cescatti, A., Chen, J., de Jeu, R., Dolman, A.J., Eugster, W., Gerten, D., Gianelle, D., Gobron, N., Heinke, J., Kimball, J., Law, B.E., Montagnani, L., Mu, Q., Mueller, B., Oleson, K., Papale, D., Richardson, A.D., Roupsard, O., Running, S., Tomelleri, E., Viovy, N., Weber, U., Williams, C., Wood, E., Zaehle, S., Zhang, K., 2010. Recent decline in the global land evapotranspiration trend due to limited moisture supply. Nature 467 (October (7318)), 951–954.

Kikuzawa, K., Lechowicz, M., 2011. Ecology of Leaf Longevity, Ecological Research Monographs. Springer-Verlag, Berlin.

Kitajima, K., Mulkey, S., Samaniego, M., Wright, S., 2002. Decline of photosynthetic capacity with leaf age and position in two tropical pioneer tree species. American Journal of Botany 89 (December (12)), 1925–1932.

Kitajima, K., Mulkey, S., Wright, S., 1997. Decline of photosynthetic capacity with leaf age in relation to leaf longevities for five tropical canopy tree species. American Journal of Botany 84 (May (5)), 702–708.

Kitajima, K., Mulkey, S., Wright, S., 1997. Seasonal leaf phenotypes in the canopy of a tropical dry forest: photosynthetic characteristics and associated traits. Oecologia 109 (February (4)), 490–498.

Laclau, J.P., Almeida, J.C.R., Goncalves, J.L.M., Saint-Andre, L., Ventura, M., Ranger, J., Moreira, R.M., Nouvellon, Y., 2009. Influence of nitrogen and potassium fertilization on leaf lifespan and allocation of above-ground growth in eucalyptus plantations. Tree Physiology 29 (1), 111–124.

Laclau, J.P., Bouillet, J.P., Ranger, J., 2000. Dynamics of biomass and nutrient accumulation in a clonal plantation of eucalyptus in Congo. Forest Ecology and Management 128 (3), 181–196.

Laclau, J.P., Ranger, J., Goncalves, J.L.D., Maquere, V., Krusche, A.V., M'Bou, A.T., Nouvellon, Y., Saint-Andre, L., Bouillet, J.P., Piccolo, M.D., Deleporte, P., 2010. Biogeochemical cycles of nutrients in tropical eucalyptus plantations main features shown by intensive monitoring in Congo and Brazil. Forest ecology and management 259 (9), 1771–1785.

le Maire, G., Marsden, C., Verhoef, W., Ponzoni, F.J., Lo Seen, D., Begue, A., Stape, J.-L., Nouvellon, Y., 2011. Leaf area index estimation with MODIS reflectance time series and model inversion during full rotations of eucalyptus plantations. Remote Sensing of Environment 115 (2), 586–599.

le Maire, G.l., Nouvellon, Y., Christina, M., Ponzoni, F.J., Goncalves, J.L., Bouillet, J., Laclau, J.-P., 2013. Tree and stand light use efficiencies over a full rotation of single- and mixed-species eucalyptus grandis and acacia mangium plantations. Forest Ecology and Management 288, 31–42.

Lebourgeois, F., Pierrat, J.C., Perez, V., Piedallu, C., Cecchini, S., Ulrich, E., 2008. Phenological timing in French temperate forests – a study on stands in the RENECOFOR network. Revue Forestiere Francaise 60 (3).

Lowman, M.D., Heatwole, H., 1992. Spatial and temporal variability in defoliation of Australian eucalypts. Ecology 73 (1), 129–142.

Marsden, C., Nouvellon, Y., Laclau, J.-P., Corbeels, M., McMurtrie, R.E., Stape, J., Epron, D., le Maire, G., 2013. Modifying the g'day process-based model to simulate the spatial variability of eucalyptus plantation growth on deep tropical soils. Forest Ecology and Management 301 (SI), 112–128.

Nouvellon, Y., Begue, A., Moran, M.S., Lo Seen, D., Rambal, S., Luquet, D., Chehbouni, G., Inoue, Y., 2000. Par extinction in shortgrass ecosystems: effects of clumping, sky conditions and soil albedo. Agricultural and Forest Meteorology 105 (1/3), 21–41.

Nouvellon, Y., Laclau, J.P., Epron, D., Kinana, A., Mabiala, A., Roupsard, O., Bonnefond, J.M., le Maire, G., Marsden, C., Bontemps, J.D., Saint-Andre, L., 2010. Within-stand and seasonal variations of specific leaf area in a clonal eucalyptus plantation in the Republic of Congo. Forest Ecology and Management 259 (9), 1796–1807.

Oja, T., Arp, P.A., 1997. A forest soil vegetation atmosphere model (forsva). 2. Application to northern tolerant hardwoods. Ecological Modelling 95 (2–3), 225–247.

Olofsson, P., 1996. General branching processes with immigration. Journal of Applied Probability 33 (4), 940–948.

Pook, E.W., 1984a. Canopy dynamics of eucalyptus maculata hook. 1. Distribution and dynamics of leaf populations. Australian Journal of Botany 32 (4), 387–403.

Pook, E.W., 1984b. Canopy dynamics of eucalyptus maculata hook. 2. Canopy leaf-area balance. Australian Journal of Botany 32 (4), 405–413.

Pook, E.W., 1985. Canopy dynamics of eucalyptus maculata hook. 3. Effects of drought. Australian Journal of Botany 33 (1), 65–79.

Pook, E.W., 1986. Canopy dynamics of eucalyptus maculata hook. 4. Contrasting responses to 2 severe droughts. Australian Journal of Botany 34 (1), 1–14.

Pook, E.W., Gill, A.M., Moore, P.H.R., 1997. Long-term variation of litter fall, canopy leaf area and flowering in a eucalyptus maculata forest on the south coast of New South Wales. Australian Journal of Botany 45 (5), 737–755.

Pornon, A., Marty, C., Winterton, P., Lamaze, T., 2011. The intriguing paradox of leaf lifespan responses to nitrogen availability. Functionnal Ecology 25 (August (4)), 796–801.

Reich, P., Uhl, C., Walters, M., Prugh, L., Ellsworth, D., 2004. Leaf demography and phenology in Amazonian rain forest: a census of 40 000 leaves of 23 tree species. Ecological Monographs 74 (February (1)), 3–23.

Reyer, C.P.O., Leuzinger, S., Rammig, A., Wolf, A., Bartholomeus, R.P., Bonfante, A., de Lorenzi, F., Dury, M., Gloning, P., Abou Jaoude, R., Klein, T., Kuster, T.M., Martins, M., Niedrist, G., Riccardi, M., Wohlfahrt, G., de Angelis, P., de Dato, G., Francois, L., Menzel, A., Pereira, M., 2013. A plant's perspective of extremes: terrestrial plant responses to changing climatic variability. Global Change Biology 19 (January (1)), 75–89.

Richardson, A.D., Keenan, T.F., Migliavacca, M., Ryu, Y., Sonnentag, O., Toomey, M., 2013. Climate change, phenology, and phenological control of vegetation feedbacks to the climate system. Agricultural and Forest Meteorology 169 (February), 156–173.

Roetzer, T., Leuchner, M., Nunn, A.J., 2010. Simulating stand climate, phenology, and photosynthesis of a forest stand with a process-based growth model. International Journal of Biometeorology 54 (July (4)), 449–464.

Roupsard, O., Dauzat, J., Nouuellon, Y., Deueau, A., Feintrenie, L., Saint-Andre, L., Mialet-Serra, I., Braconnier, S., Bonnefond, J.-M., Berbigier, P., Epron, D., Jourdan, C., Navarro, M., Bouillet, J.-P., 2008. Cross-validating sun-shade and 3d models of light absorption by a tree-crop canopy. Agricultural and Forest Meteorology 148 (April (4)), 549–564.

Saint-André, L., 2013, April. Intégration des cycles biogéochimiques dans les modèles de croissance à base dendrométrique. concepts - forces et limites de l'approche. Habiliation à diriger la recherche – Ecole doctorale RP2E.

Saint-André, L., Laclau, J.-P., Bouillet, J.-P., Deleporte, P., Miabala, A., Ognouabi, N., Bailleres, H., Nouvellon, Y., Moukini, R., 2002. Integrative modelling approach to assess the sustainability of the eucalyptus plantations in Congo. Fourth Workshop.

Saint-André, L., Laclau, J.P., Deleporte, P., Gava, J.L., Goncalves, J.L.M., Mendham, D., Nzila, J.D., Smith, C., Toit, B.D., Xu, D.P., Sankaran, K.V., Marien, J.N., Nouvellon, Y., Bouillet, J.P., Ranger, J., 2008. Slash and litter management effects on eucalyptus productivity: a synthesis using a growth and yield modelling approach. In: Site Management and Productivity in Tropical Plantation Forests: Proceedings of Workshops in Piracicaba (Brazil) 22–26 November 2004 and Bogor (Indonesia), 6–9 November 2006, pp. 173–189.

Saint-André, L., M'bou, A.T., Mabiala, A., Mouvondy, W., Jourdan, C., Roupsard, O., Deleporte, P., Hamel, O., Nouvellon, Y., 2005. Age-related equations for above- and below-ground biomass of a eucalyptus hybrid in congo. Forest Ecology and Management 205 (1–3), 199–214.

Sainte-Marie, J., Henrot, A., Saint-André, L., Barrandon, M., Nouvellon, Y., Roupsard, O., Laclau, J.P., 2012. Modeling the environmental and seasonal influence on canopy dynamic and litterfall of even-aged forest ecosystems by a model coupling growth and yield and process-based approaches. In: Plant Growth Modeling, Simulation, Visualization and Applications: Proceedings – PMA'12, pp. 324–331.

Shuttleworth, W.J., Wallace, J.S., 1985. Evaporation from spare crops – an energy combination theory. Quarterly Journal of the Royal Meteorological Society 111 (469), 839–855.

Silva, A.L.L., da Oliveira, Y., de Alcantara, G.B., de Santos, M., dos Quoirin, M., da Silva, A.L.L., de Oliveira, Y., de Alcantara, G.B., dos Santos, M., 2009. Chilling and frost tolerance in eucalypt leaves. Biociencias 17 (1), 86–90.

Stape, J., Binkley, D., Ryan, M., 2004. Eucalyptus production and the supply, use and efficiency of use of water, light and nitrogen across a geographic gradient in brazil. Forest Ecology and Management 193 (1–2), 17–31.

Stoeckli, R., Rutishauser, T., Dragoni, D., O'Keefe, J., Thornton, P.E., Jolly, M., Lu, L., Denning, A.S., 2008. Remote sensing data assimilation for a prognostic phenology model. Journal of geophysical research-biogeosciences 113 (G4), G04021.

Sverdrup, H., Thelin, G., Robles, M., Stjernquist, I., Sorensen, J., 2006. Assessing nutrient sustainability of forest production for different tree species considering ca, mg, k, n and p at Bjornstorp Estate, Sweden. Biochemistry 81 (2), 219–238.

Van Veldhuizen, D.A., Lamont, G.B., 2000. Multiobjective evolutionary algorithms: analyzing the state-of-the-art. Evolutionary Computation 8 (2), 125–147.

Vincent, G., 2006. Leaf life span plasticity in tropical seedlings grown under contrasting light regimes. Annals of Botany 97 (2), 245–255.

Vitasse, Y., Delzon, S., Bresson, C.C., Michalet, R., Kremer, A., 2009a. Altitudinal differentiation in growth and phenology among populations of temperate-zone tree species growing in a common garden. Canadian Journal of Forest Resarch – Revue Canadienne de Recherche Forestière 39 (7), 1259–1269.

Vitasse, Y., Delzon, S., Dufrene, E., Pontailler, J.Y., Louvet, J.M., Kremer, A., Michalet, R., 2009. Leaf phenology sensitivity to temperature in European trees: do within-species populations exhibit similar responses? Agricultural and Forest Meteorology 149 (5), 735–744.

Vitasse, Y., Porte, A.J., Kremer, A., Michalet, R., Delzon, S., 2009c. Responses of canopy duration to temperature changes in four temperate tree species: relative contributions of spring and autumn leaf phenology. Oecologia 161 (1), 187–198.

Wallman, P., Svensson, M.G.E., Sverdrup, H., Belyazid, S., 2005. Forsafe – an integrated process-oriented forest model for long-term sustainability assessments. Forest Ecology and Management 207 (1–2), 19–36.

Whitehead, D., Beadle, C., 2004. Physiological regulation of productivity and water use in eucalyptus: a review. Forest Ecology and Management 193 (May (1–2)), 113–140.

Wright, I., Reich, P., Cornelissen, J., Falster, D., Groom, P., Hikosaka, K., Lee, W., Lusk, C., Niinemets, U., Oleksyn, J., Osada, N., Poorter, H., Warton, D., Westoby, M., 2005. Modulation of leaf economic traits and trait relationships by climate. Global Ecology and Biogeography 14 (September (5)), 411–421.

Wright, S., Van Schaick, C., 1994. Light and phenology of tropical trees. American Naturalist 143 (1), 192–199.

Zhu, Z.X., Arp, P.A., Meng, F.R., Bourque, C.P.A., Foster, N.W., 2003a. A forest nutrient cycling and biomass model (fornbm) based on year-round, monthly weather conditions – Part II: Calibration, verification, and application. Ecological Modelling 170 (1), 13–27.

Zhu, Z.X., Arp, P.A., Meng, F.R., Bourque, C.P.A., Foster, N.W., 2003b. A forest nutrient cycling and biomass model (fornbm) based on year-round, monthly weather conditions. Part 1: Assumption, structure and processing. Ecological Modelling 169 (2–3), 347–360.